

Deactivation Behavior of Bifunctional Pt/H-Zeolite Catalysts during Cyclopentane Hydroconversion

Srikant Gopal and Panagiotis G. Smirniotis¹

Department of Chemical Engineering, University of Cincinnati, Cincinnati, Ohio 45221-0171

Received March 26, 2001; revised September 28, 2001; accepted September 28, 2001

Cyclopentane hydroconversion was used as a probe reaction to study the coking behavior of selected large-pore zeolites loaded with 0.5% Pt under identical conditions. The zeolites studied, namely, Y zeolite, zeolite beta, mordenite, LTL, and ZSM-12, were also tested at several different Si/Al ratios. The zeolite pore structure was the most important factor determining the deactivation behavior. Zeolites like Y and L that possess large cavities connected to smaller pore openings allow polyaromatic molecules to form and also trap these coke molecules to a great extent, resulting in rapid deactivation. This was confirmed by the analysis of soluble coke, which revealed the presence of large amounts of benzoperylene and coronene. Zeolite beta, which possesses an intersecting three-dimensional pore system, but no large cages, was the most stable. Apart from its pore structure, the excellent stability of the zeolite beta catalysts could also be partly attributed to the electronic state of platinum in the catalyst. The absence of aromatic compounds in the product stream and the aliphatic nature of coke indicated that the platinum in zeolite beta selectively opened the cyclopentane ring and did not dehydrogenate it, preventing the formation of cyclopentadiene that condenses via a Diels–Alder mechanism into polyaromatic coke. Mordenite and ZSM-12 showed reasonably good stability. Interestingly, the soluble coke in mordenite consisted of both polyaromatic and long-chain aliphatic compounds, indicating that the selectivity of the metal function changes with time. The amount of “hard coke” deposited in the zeolites was strongly related to the initial activity of the acid function, with the more active catalysts having a larger amount of coke. However, this trend was not followed in ZSM-12 which showed a shape-selective behavior that restricted the deposition of hard coke to a great extent. Apart from pore structure, variation of the acid site density (Si/Al ratio) affected metal dispersion and metal/acid balance and caused significant differences in the catalytic performance within a particular type of zeolite. However, the nature of the acid sites (Brønsted or Lewis) did not have a significant effect. Catalysts that had Si/Al ratios in the range 15 to 40 showed a minimum in the C_1/C_3 ratio indicating a good balance between the metallic and acidic functions and showed good time stability. © 2002 Elsevier Science

INTRODUCTION

Deactivation due to coking is observed in all heterogeneous acid-catalyzed reactions of organic compounds. Coke formation is a major concern when using acidic zeolite catalysts, and understanding the mechanisms that control coking and its effect on catalytic properties such as activity and selectivity is essential in terms of catalyst selection and process design (1). Coke deposition in zeolites is known to be affected by its pore size, pore structure, and acidity characteristics. Rollmann and Walsh (2–4) were among the earliest researchers to show not only that coke formation is a shape-selective reaction but also that coke yield in molecular shape-selective zeolites (small and intermediate pore) is at least an order of magnitude lower than that in the large-pore materials. The low coking rate found on H-ZSM-5 was first related only to the shape-selective nature of its pores, but later it was also attributed to the relatively low density of its acid sites (5). It is difficult to distinguish the effect of acidity from that of pore structure, but zeolites with high acid site densities were generally found to deactivate faster due to higher conversion severity, which resulted in higher coke yields. In reforming reactions carried over bifunctional catalysts, the coke precursors are hydrogenated over the metal function and get desorbed. The net effect is beneficial, as the coke production rate is several orders of magnitude lower than that over an acidic catalyst (5). Investigations of naphtha reforming over bifunctional catalysts revealed that the five-carbon-ring hydrocarbons, primarily cyclopentane, were the most important coke precursors (6–8). The coke formation in these reforming catalysts was also a bifunctional reaction requiring both the dehydrogenation capacity of the metallic function and the condensing capacity of the acidic function.

In this paper, the coking behavior of various large-pore zeolites, namely, Y zeolite, zeolite beta, L zeolite, mordenite, and ZSM-12, was studied for the hydroconversion of cyclopentane. The zeolites chosen combine a variety of pore architectures with different pore sizes and also different dimensionalities. Each zeolite was studied at several different Si/Al ratios, and we have attempted to cover a wide

¹ To whom correspondence should be addressed. E-mail: panagiotis.smirniotis@uc.edu.



range of Si/Al ratios for each zeolite. Using the coke precursor, cyclopentane, as a probe molecule allowed us to identify stable catalytic systems and to better understand the factors affecting coke formation. The study showed that three-dimensional zeolites without supercages like zeolite beta with the right level of acid site density and metal loading were the best catalysts for reforming-type reactions in terms of time stability. Acid site density affected catalytic performance to a great extent, and an optimum range for obtaining good stability was identified.

EXPERIMENTAL

Catalyst Preparation

The beta and ZSM-12 zeolites used in this study were synthesized hydrothermally from the corresponding aluminosilicate gels. The starting recipe for the synthesis of ZSM-12 was example IV in the original patent (9), which was optimized following the results reported by Ernst *et al.* (10). Tetraethylammonium hydroxide (Fluka, 40% in water) was used as the template, colloidal silica (LUDOX HS-40, DuPont) was used as the silica source, and sodium aluminum oxide (Alfa Aesar, Technical grade) was used

as the aluminum source. The gel was prepared by mixing the reagents in appropriate proportions and transferring them to a Teflon-lined autoclave. Crystallization was done at 160°C for ZSM-12. Zeolite beta was synthesized using the same starting materials as those used in ZSM-12 synthesis, but with a higher aluminum content in the gel, and the crystallization was carried out at a temperature of 140°C.

A series of Y zeolites with Si/Al ratios ranging from 2.5 to 40 were obtained from Zeolyst International (formerly PQ Corporation). Zeolyst International prepared the higher Si/Al samples by controlled steam treatment followed by lean acid leaching of the parent Y faujasite. A list of zeolites used in this study, their physical properties, and details of the dealumination procedures are given in Table 1. Mordenite and L zeolite were kindly donated to us by UOP. Dealumination of mordenite was carried out in a three-necked flask under reflux conditions, using HCl as the dealuminating agent. Different Si/Al ratios were obtained by varying the concentration of HCl. The parent L zeolite underwent significant structure destruction when dealuminated with ammonium hexafluorosilicate (AHF) and *it was* destroyed completely when treated with even very dilute HCl. Therefore careful steaming followed by AHF treatment was used

TABLE 1

Properties of the Large-Pore Zeolites Used in the Present Study

Zeolite and pore structure	Pore structure—schematic	Zeolite samples ^a	Preparation method	Percentage crystallinity
Y 3-D, 7.4 Å		Y-2.5 ^b	Parent NaY	100
		Y-6 ^b	Steaming + mild acid leaching	83
		Y-15 ^b	Steamed twice + strong acid leaching	70
		Y-30 ^b	Steamed twice + strong acid leaching	72
		Y-40 ^b	Steamed twice + strong acid leaching	61
Zeolite beta 3-D, 7.3 × 6.5 and 5.6 × 5.6 Å		Beta-8.5	Synthesized	100
		Beta-15	Synthesized	100
		Beta-30	Synthesized	100
Mordenite 2-D, 7 × 6.5 and 5.7 × 2.6 Å		Mor-10	As received	100
		Mor-25	0.5 N HCl dealuminated	109
		Mor-35	1 N HCl dealuminated	109
LTL 1-D, 7.1 Å		LTL-3.5	As received	100
ZSM-12 1-D, 5.6 × 6.1 Å		ZSM-12-38	Synthesized	100
		ZSM-12-43	Synthesized	100
		ZSM-12-58	Synthesized	100
		ZSM-12-80	Synthesized	100

^a Numbers after zeolite name indicate Si/Al ratio.

^b Si/Al ratio reported by company.

for the dealumination of L zeolite. The steam treatment was performed at 620°C for 4 h, and the zeolite was further dealuminated using AHF in a three-necked flask under reflux conditions. The zeolites synthesized in our laboratory were calcined in air at 520°C for 4 h to burn the occluded template and obtain the sodium form. Ammonium forms of the zeolites were obtained by cation exchange with 2 N NH₄Cl solution at 90°C for 4 h. Finally, the zeolites were converted to their protonated forms by calcination in air at 500°C for 1 h. Platinum was loaded on the protonated form of the catalysts by wet impregnation using H₂PtCl₆ (Aldrich 8 wt% solution in water). A final Pt loading of 0.5 wt% was achieved. The impregnated catalysts were dried overnight in an oven at 120°C. Reduction of the catalysts to disperse the metal was done *in situ* before starting the reaction, and the reduction conditions were chosen so that a relatively high dispersion of the metal was obtained.

Characterization

X-ray diffraction (XRD). XRD was employed for both the identification of the synthesized zeolite phases and the quantification of the crystallinities of dealuminated zeolites. The XRD patterns were collected with a Siemens powder X-ray diffractometer using CuK α radiation. The crystallinity of dealuminated zeolites was estimated based on the heights of the main crystallographic peaks of each zeolite.

Elemental analysis. The bulk Si/Al ratios of the zeolites were determined by inductively coupled plasma (ICP) spectroscopy. The method described by Mackey and Murphy (11) was used for the analysis. The technique involved dispersing a small amount of the zeolite powder in distilled water and directly injecting the suspension into the ICPEs plasma using a high-solids nebulizer. The signal was then compared to that from a set of combined liquid standards. The aspiration rate and solid concentration of the suspension were not critical to precision, as we were interested only in determining the relative amounts (ratios) of the elements.

Acidity characterizations. NH₃ stepwise temperature-programmed desorption (STPD) was used for the measurement of acid site density. When STPD was coupled with FT-IR, quantitative characterization of the Brønsted and Lewis acid sites was obtained (12). For the STPD experiments, 50 mg of the protonated zeolite was loaded into the middle of a 6-mm-i.d. horizontal tube. Each sample was first cleaned by passing He at 550°C for 1 h. The sample was then cooled to 150°C, and anhydrous ammonia (4% in He) was admitted to the bed for 1 h to ensure saturation of all the zeolite acid sites. Helium was then sent to the bed to remove excess ammonia and any physisorbed ammonia. This step was maintained until no ammonia desorption was observed. Then the STPD profile, which consisted of

five sets of ramps and isothermal steps, was started. The desorption experiment followed a profile which started at 150°C and ended at 540°C. Detection of ammonia was carried out using a thermal conductivity detector (TCD). The same procedure was followed for the characterization of deactivated catalysts.

FT-IR spectroscopy was used to assign the ammonia desorption peaks to Brønsted or Lewis acid sites. Thin wafers of the protonated form of each zeolite sample were prepared by pressing about 5 mg of dry powder. The wafer was placed in a bakeable IR cell with CaF₂ windows and equipped for continuous flow of gases. The spectra were recorded using a Bio-Rad FTS-40 spectrophotometer. The procedure used was described in detail previously (12).

Hydrogen chemisorption. The dispersion of platinum on the catalysts was determined using hydrogen chemisorption. The analysis was carried out using a Micromeritics accelerated surface area porosimetry and chemisorption system (ASAP 2010 Chemi). Before analysis the catalyst was first oxidized *in situ* at 450°C for 1 h and then reduced at 450°C for 1 h. It should be noted that the oxidation and reduction conditions were the same as those used to activate the catalyst before the reaction. After reduction, the catalyst was cooled down to 100°C, and the isotherm was measured with the hydrogen pressure ranging from 75 to 240 mm Hg. Blank experiments using the zeolite showed that no adsorption of hydrogen took place on the support. Metal dispersion was calculated by extrapolating the isotherm to zero pressure and assuming a H : Pt stoichiometry of 1 : 1.

Catalytic Experiments

Cyclopentane (CP)(Aldrich, 99%) was used as the probe molecule for studying time-on-stream behavior of the catalysts because it is known to be an “efficient” molecule for coke formation among naphthenes. Coke formation from CP is a bifunctional reaction requiring the dehydrogenating action of the metal to produce cyclopentadiene, which then condenses over the acid site via a Diels–Alder-type mechanism to give polycyclic hydrocarbons (13, 8). Due to this reason we decided to use CP as the feed to study several Pt/H zeolites under severe coking conditions.

The catalytic experiments were carried out in a flow reactor system using a 6.25-mm-o.d. 316 stainless-steel reactor. In all the experiments 100 mg of fresh catalyst was loaded on top of a glass wool plug. The catalysts were activated *in situ* by oxidation with high-purity oxygen for 1 h at 450°C, followed by purging with high-purity He for 15 min. The reduction of the catalyst was carried out at 450°C in high-purity H₂ for 1 h at atmospheric pressure. H₂ was provided from the gas cylinder to the reactor while pressure regulation was achieved with a back-pressure regulator, placed at the exit of the reactor tube. The feed was introduced at

a predetermined flow rate into a heated line going to the reactor, using an ISCO 100DM syringe pump.

Product identification was accomplished using a high-resolution gas chromatograph (GC) (Hewlett–Packard, 5890 Series II) equipped with a mass spectrometer (MS) (Hewlett–Packard, 5972 Series II). The reactor effluent stream was sent to the GC/MS for analysis through a heated line (about 180°C). The GC/MS was attached to a PC unit for data acquisition and processing. The GC was equipped with a high-performance capillary column (SUPELCO Petrocol DH50.2, fused silica with bonded dimethylsiloxane, 0.2 mm i.d., 50-m flow length, and 0.5- μ m film thickness). By optimizing the temperature profile of the GC oven and flow of carrier gas, efficient separation of all the products of the reaction was achieved.

The reaction was carried out at a temperature of 410°C and 100 pounds per square inch gauge (psig) (6.8 atm) pressure. The weight-hourly space velocity (WHSV) was set at 3 h⁻¹, and the H₂/hydrocarbon molar ratio was 9 for the majority of the experiments. The reaction temperature was fixed at 410°C to work in the range close to industrial reforming conditions. Operation at this temperature allowed us to follow the deactivation profile of each catalyst clearly. All experiments were carried out for 100 h on stream.

Coke Characterization

Thermogravimetric analysis. The used catalysts were collected after the reaction and stored in sealed containers for coke analysis. The amount of “hard” coke deposited on the catalysts was determined by thermogravimetric analysis (TGA) using a Perkin–Elmer TGA-7 system. For this analysis, the deactivated catalysts were first cleaned by heating the catalyst at a rate of 10°C/min in nitrogen flow to a temperature of 550°C and holding for 1 h. The catalyst was then cooled to 100°C and held for 1 h to allow the weight to become constant. The coke remaining on the catalyst was then combusted using high-purity oxygen at a temperature increase rate of 10°C/min to a final temperature of 550°C, and the weight change of the catalyst during oxidation was followed. After the oxidation step, the catalyst was cooled back to 100°C, and the difference in weight was measured. The ratio of this weight difference to the weight of the catalyst (at 100°C, after the cleaning step) yielded the weight percent of coke in the catalyst.

GC/MS analysis of soluble coke. For analysis of the coke composition, the deactivated catalysts recovered after the reaction were dissolved in 49% hydrofluoric acid, and the soluble coke was extracted using methylene chloride (CH₂Cl₂, Fisher, 99.9+wt%). The coke extract was then concentrated by evaporating the solvent. The soluble coke components were analyzed using a Shimadzu GC-17A gas chromatograph and GCMS-QP5050A mass spectrometer system. Separation was achieved using a 30-m-long, 0.25-mm-i.d. Restek XTI-5 column.

Temperature-programmed oxidation (TPO). TPO profiles for the deactivated catalysts were obtained by heating the catalysts at 5°C/min in a high-purity stream of oxygen (4.2% O₂ in helium). The CO₂ evolved was followed using a MKS PPT-RGA quadrupole mass spectrometer.

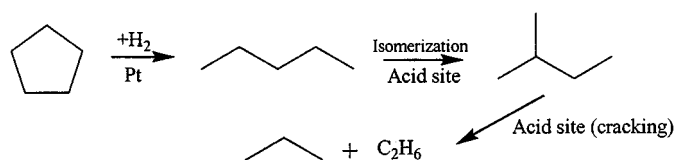
RESULTS AND DISCUSSION

Time-on-Stream Behavior

Most catalysts used in heterogeneous catalytic processes experience a decrease in activity over a period of time. The time required for the activity of a catalyst to fall to an undesirable level depends on several factors. In acidic zeolites this occurs due to deposition of coke. The cost of catalyst deactivation is very high in industrial processes, therefore catalysts with superior time stability are very valuable. Large-pore zeolites, especially high-silica zeolites, are attractive catalysts for reforming-type reactions, and the time stability of these catalysts would be one of the important factors in determining their use in these reactions. The time-on-stream behavior of selected large-pore zeolites was examined in this study, and the deactivation behavior of these zeolites is discussed in the following sections.

The activities of the catalysts were monitored as a function of the time on stream. The catalysts usually lost activity rapidly during the initial few hours, and the conversion then reached a constant “level-off” value after a few hours on stream. The reaction was stopped after the catalyst completed 100 h on stream, and the deactivated samples were recovered and stored for further analysis. CP conversion was calculated using the amount of unreacted CP and the CP fed to the reactor. Product selectivities are defined as the concentration of the individual component over the concentration of all products in the effluent stream.

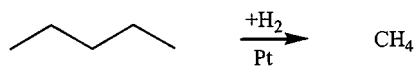
Based on the product distributions obtained, the main reactions occurring over the various catalysts could be determined. This is presented prior to the description of the TOS behavior of the various catalysts as it assists the reader in better understanding the deactivation behavior. The main reaction occurring on the catalysts is the ring opening of the cyclopentane over the metal function to produce *n*-pentane, which is further isomerized over the acid site into 2-methylbutane and cracked into smaller alkanes (Scheme 1).



SCHEME 1

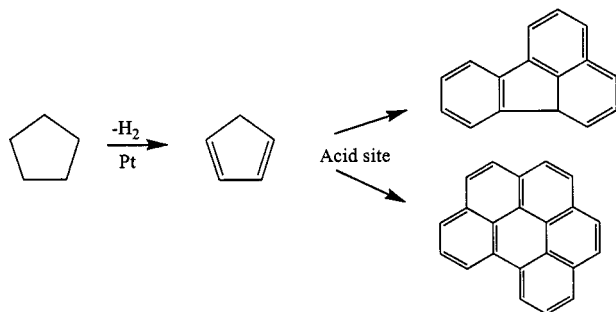
A large fraction of methane is also observed in the product stream. Most of the methane is produced due to

hydrogenolysis of the alkanes over the metal function. This reaction could be represented as shown in Scheme 2.



SCHEME 2

Cyclopentane hydroconversion experiments were carried out with the individual metal and acid functions to further clarify their roles. The Pt/SiO₂ catalyst showed a stable conversion of 50% with pentane and methane as the major products. The acidic zeolite gave all the cracked products, but the conversion was very low. This also shows that the hydroconversion of cyclopentane proceeds efficiently only over a bifunctional catalyst. The other reaction taking place over the catalysts is the conversion of cyclopentane into coke. As mentioned earlier, coke formation results from cyclopentadiene (CPde) which is formed by dehydrogenation of CP on the metallic function of the catalyst. This CPde ring (Scheme 3) has a conjugate double bond, which is very reactive and can condense with another CPde ring by a Diels–Alder-type condensation giving an indenic structure leading to polycyclic hydrocarbons (8).



SCHEME 3

Molecules larger than cyclopentane such as C₆ alkanes, methyl cyclopentane, and aromatics were also observed in small amounts over some of the catalysts. These were formed due to the cracking of the condensed aromatic products and the further transformations of the products obtained from this cracking. The variation of catalytic activities and product distributions with time on stream is discussed in detail in the following sections for the specific zeolites.

Y zeolite. Cyclopentane hydroconversion was studied on five different Y zeolite samples with different levels of dealumination. The time-on-stream behavior of these samples is shown in Fig. 1. A very fast drop in activity occurs during the initial few hours after which it reaches a constant value. A trend can also be observed in the stability of the catalysts, which improve with increase in the Si/Al ratio of the zeolite. We can also see two distinct kinds of behavior: the aluminum-rich samples deactivate to a great extent,

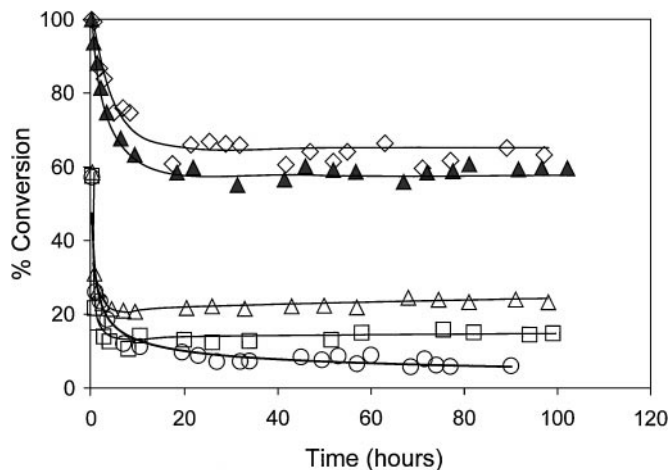


FIG. 1. Time-on-stream behavior of the series of Y zeolites studied. \diamond , Y-40; \blacktriangle , Y-30; \triangle , Y-15; \square , Y-6; \circ , Y-2.5. WHSV = 3 h⁻¹, H₂/CP (molar) = 9, total pressure = 100 psig, and $T = 410^\circ\text{C}$, and 0.5% Pt loading.

while the highly dealuminated Y-30 and Y-40 samples deactivate to some extent but maintain reasonably good activity. Deactivation is also much more rapid in the aluminum-rich zeolites. As already established, coke trapping is the primary reason for the deactivation of Y zeolites (14, 15). Y faujasite has a three-dimensional network of 7.4 Å pores connected to 12.4 Å supercages. These large cages allow the formation of bulky coke molecules larger than the pore size, which then get trapped in the cages, blocking access of reactants to other active sites and resulting in rapid deactivation.

The large amount of “hard” coke deposited inside the zeolites after the reaction, determined by TGA (Fig. 2), confirms that coking and coke trapping occur to a major extent in the cages of zeolite Y. The amount of coke appears to reach a maximum in the Y-6 sample. Y-2.5 has a lower coke content than Y-6 or Y-15 even though it is

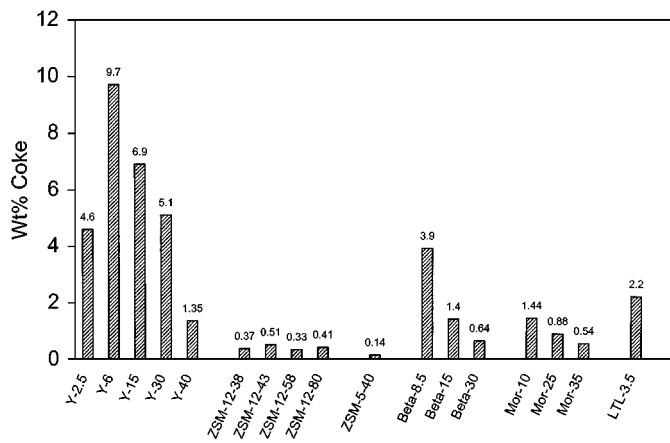


FIG. 2. Amount of “hard coke” deposited in the various zeolites after 100 h on stream. Hard coke here refers to coke remaining in the catalyst after purging with nitrogen at 550°C for 1 h.

TABLE 2
Product Selectivities (mol%) over the Pt/Y Zeolite Catalysts Studied^a

	Initial (20 min)					Level-off stage				
	Y-2.5	Y-6	Y-15	Y-30	Y-40	Y-2.5	Y-6	Y-15	Y-30	Y-40
CP conversion	57.3	57.6	97.2	99.9	99.9	7.5	15.3	19.8	58.5	61.3
Methane	10.8	20.8	38.3	40.4	32.7	35.6	39.0	18.5	11.1	5.9
Ethane	1.4	6.9	6.5	17.7	14.7	1.9	1.4	1.0	1.7	1.0
Propane	4.0	21.0	11.6	18.5	18.6	3.1	2.3	1.6	2.3	1.4
2-Methylpropane	3.6	10.7	4.8	3.6	3.4	0.4	0.7	0.7	0.5	0.3
Butane	2.1	9.9	5.1	8.6	12.1	2.1	0.9	0.9	1.5	1.0
2,2-Dimethylpropane	0.0	0.0	0.3	0.3	0.4	0.0	0.0	0.0	0.0	0.0
2-Methylbutane	42.3	14.0	19.7	7.1	10.4	3.7	14.3	21.5	37.5	37.2
Pentane	33.6	9.3	13.0	3.9	7.7	51.6	39.1	52.2	44.8	52.6
Cyclopentene	0.0	0.1	0.0	0.0	0.0	1.1	1.7	0.6	0.1	0.0
2-Methylpentane	0.4	0.6	0.3	0.0	0.0	0.0	0.0	1.5	0.2	0.3
3-Methylpentane	0.3	0.3	0.2	0.0	0.0	0.2	0.1	0.4	0.2	0.2
Hexane	0.3	0.3	0.1	0.0	0.0	0.1	0.0	0.2	0.1	0.1
Methyl cyclopentane	0.3	1.2	0.0	0.0	0.0	0.0	0.5	0.5	0.1	0.0
Benzene	0.7	3.0	0.0	0.0	0.0	0.0	0.0	0.3	0.1	0.0
Toluene	0.2	1.6	0.0	0.0	0.0	0.0	0.0	0.0	0.0	0.0

^a WHSV = 3 h⁻¹, H₂/CP (molar) = 9, total pressure = 100 psig, T = 410°C, and 0.5% Pt loading.

completely deactivated. This suggests that a rapid pore mouth plugging might be occurring in the Y-2.5 catalyst. The coke contents can be explained based on the activity of the acid function. The conversion and coking severities are higher in the samples in which the acid function is more active, resulting in the formation and deposition of larger amounts of coke. The steam dealumination procedure employed in the preparation of the Y-6 sample deposits a large amount of aluminum at the surface. From XPS analyses we observed a much higher concentration of aluminum at the surface compared to the bulk. Similar observations were made by others (16), and the high concentration of the surface aluminum was shown to enhance the activity of the acid function severalfold. Therefore even though the Y-6 and Y-15 catalysts have lower acid site densities than Y-2.5, their acidic functions are more active, causing the formation and deposit of a larger amount of coke.

Table 2 shows the product selectivities for the Y zeolite samples at the initial stage and after the conversion reaches a constant value. Again, the distinction between the low Si/Al samples and the high Si/Al samples can be observed. In the aluminum-rich catalysts a large amount of products obtained due to isomerization and cracking of *n*-pentane can be observed at the initial stages of the reaction. However, only pentane and methane are the significant products after a few hours on stream, which indicates that the acid function has undergone complete deactivation. The remaining activity is due to the metal present at the external surface of the catalyst. Y-6 and Y-15 deactivate rapidly, but the conversion stabilizes at a higher value than Y-2.5. In Y-6 and Y-15 a significant amount of 2-methylbutane is also observed at the level-off stage, which indicates that some

acid sites are still active. In both catalysts, the surface is enriched in aluminum, which is again probably responsible for the residual isomerization activity in the deactivated catalyst. The performance of Y-30 and Y-40 catalysts is very similar. The product distribution at the flat portion of the curve shows a large fraction of methylbutane and also some cracked products, indicating that many acid sites which are capable of isomerization and cracking remain active.

The acidity characteristics for the zeolites studied (determined by STPD and FTIR) are given in Table 3. It can be seen that for the series of Y zeolite samples there is a considerable variation in the ratio of the number of Brønsted to Lewis sites. However, this does not appear to affect the trends in deactivation behavior of the catalysts. The data indicate that only the acid site densities have an effect on the stability of the catalysts, while the effect of the type of acid site present is insignificant. The metal dispersions for the catalysts determined by hydrogen chemisorption are also given in Table 3. Very high dispersions were obtained for the two highly dealuminated Y zeolite samples, whereas the dispersions were substantially lower for the aluminum-rich samples. Thus, the lower acid site density, in addition to decreasing the severity of coking, also results in a better dispersion of the metal and gives catalysts with better stability. Figure 3 shows the fraction of acid sites remaining in the catalysts after the reaction as determined by NH₃ STPD. Only about 25% of the acid sites are accessible to ammonia in the aluminum-rich catalysts, whereas about 75% of the sites are accessible in the highly dealuminated sample.

In Y-30 and Y-40 both metal and acid sites are very active initially resulting in almost complete conversion of cyclopentane. The selectivity for methane is very high initially

TABLE 3

Acidity Characteristics^a and Metal Dispersion (0.5% Pt) for the Zeolites Studied

Zeolite	No. of acid sites (mmol/g)	No. of Brønsted sites (mmol/g)	No. of Lewis sites (mmol/g)	No. of Brønsted/No. of Lewis	Percentage Pt dispersion
Y-2.5	2.21	0.78	1.43	0.55	36
Y-6	0.81	0.31	0.50	0.62	32
Y-15	0.79	0.65	0.14	4.64	43
Y-30	0.40	0.14	0.26	0.54	116
Y-40	0.21	0.17	0.04	4.25	82
Beta-8.5	0.99	0.76	0.23	3.30	46
Beta-15	0.69	0.37	0.32	1.16	84
Beta-30	0.49	0.34	0.15	2.27	75
Mor-10	1.31	0.51	0.80	0.64	58
Mor-25	0.67	0.13	0.54	0.24	78
Mor-35	0.51	0.25	0.26	0.96	63
LTL-3.5	1.16	0.28	0.88	0.24	78
ZSM-12-38	0.36	0.23	0.13	1.77	70
ZSM-12-43	0.34	0.29	0.05	5.80	70
ZSM-12-58	0.25	0.07	0.18	0.39	86
ZSM-12-80	0.22	0.18	0.04	4.50	57

^aAcidity characterizations (NH₃ STPD and FT-IR) were performed using the protonated form of the zeolite before platinum was loaded.

indicating that the metal function is highly active. It is possible that the activities of metal and acid functions are more balanced in the high Si/Al samples. To check this we examined the molar ratio of C₁/C₃ hydrocarbons produced over each zeolite as a function of time. Parera *et al.* (17) employed this ratio as an approximate measure of the activity of the metal function to the activity of the acidic function. This ratio was also used in some industrial processes to follow the balance between the activities of both functions. As mentioned earlier, a separate set of experiments carried out using monofunctional catalysts, i.e., Pt loaded on SiO₂

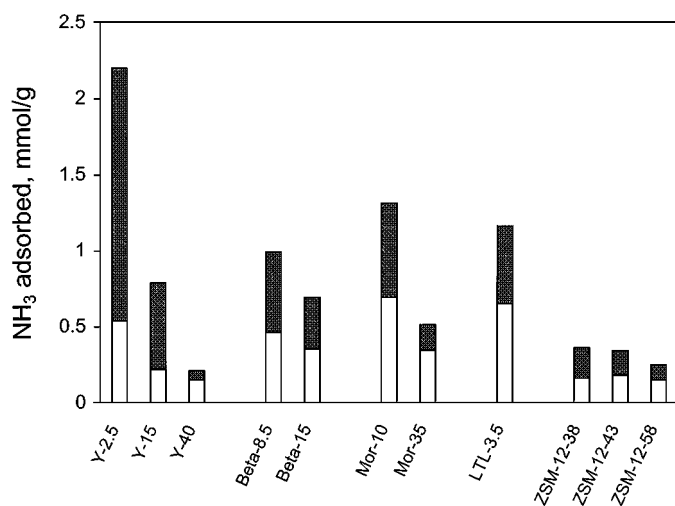


FIG. 3. Number of acid sites accessible to ammonia in the fresh and deactivated catalysts as determined by NH₃ STPD. The total height of the bar (shaded + unshaded) indicates the total acidity of the fresh catalyst. The unshaded portion represents the amount of acid sites accessible to ammonia in the used catalyst.

and an acidic zeolite, showed that a majority of the methane was produced by hydrogenolysis over the metal, while cracking on the acid sites produced almost all of the propane. This indicates the validity of the C₁/C₃ ratio for comparing metal/acid activity. For the Y zeolite catalysts the variation of C₁/C₃ ratio with time is shown in Fig. 4. The acid function is initially active in all the catalysts, and low C₁/C₃ ratios are obtained. Deactivation of the acid function in the aluminum-rich Y zeolites causes the C₁/C₃ ratio to increase rapidly and then to become constant when only the metal present at the surface of the catalyst is active. In the highly dealuminated catalysts, the C₁/C₃ ratio remains low indicating a better balance between the two functions.

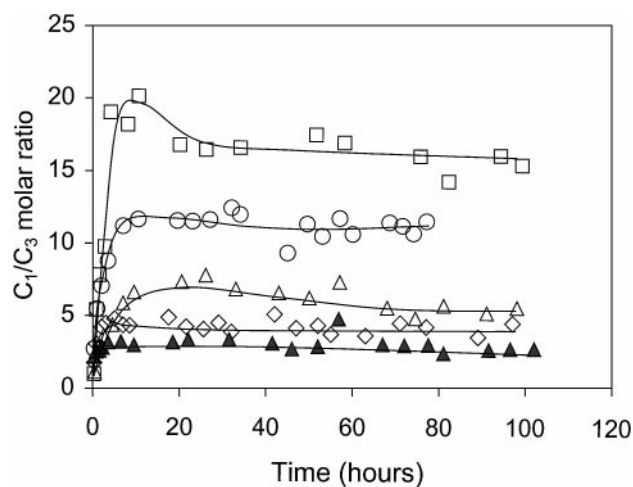
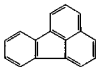
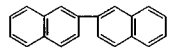
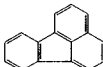
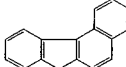
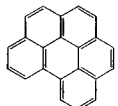
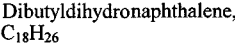
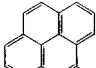
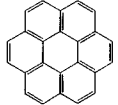
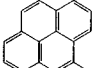
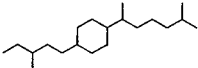
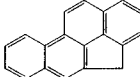
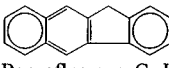
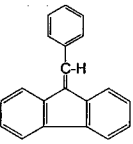
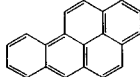
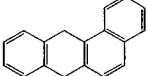


FIG. 4. Variation of the C₁/C₃ molar ratio with time for Y zeolites. □, Y-6; ○, Y-2.5; △, Y-15; ◇, Y-40; ▲, Y-30. WHSV = 3 h⁻¹, H₂/CP (molar) = 9, total pressure = 100 psig, T = 410°C, and 0.5% Pt loading.

TABLE 4
Major Components of Soluble Coke in the Zeolites Studied

Zeolites Y and L		Zeolite beta	Mordenite	
 Fluoranthene, C ₁₆ H ₁₀	 2,2-Binaphthalene, C ₂₀ H ₁₄	C ₁₆ H ₃₂ C ₁₉ H ₃₈ C ₁₉ H _{40C₂₀H₄₂ (several isomers) C₂₁H₄₄}	 Fluoranthene, C ₁₆ H ₁₀	C ₂₂ H ₂₄ 2-Phenyl hexadecane, C ₂₂ H ₃₈
 Benzofluorene, C ₁₇ H ₁₂	 Benzoperylene, C ₂₂ H ₁₂	4-Methyl-1-decenyl benzene (C ₁₇ H ₂₆) and other compounds having long alkyl chains attached to a benzene ring	 Dibutylidihydronaphthalene, C ₁₈ H ₂₆	C ₂₀ H ₄₂ (several isomers)
 Methylpyrene, C ₁₇ H ₁₂	 Coronene, C ₂₄ H ₁₂		 Methylpyrene, C ₁₇ H ₁₂	 C ₂₀ H ₄₀
 4,5-Methanochrysene, C ₁₉ H ₁₂			 Benzofluorene, C ₁₇ H ₁₂	 Benzal fluorene, C ₂₀ H ₁₄
 Benzopyrene, C ₂₀ H ₁₂			1-Hexadecene, C ₁₆ H ₃₂	3,5-Diphenyl-1-pentene, C ₁₇ H ₁₈
			Nonadecane, C ₁₉ H ₄₀	1,6-Diphenyl-1,5-hexadiene, C ₁₈ H ₁₈
			 Benzanthracene, C ₁₈ H ₁₄	

After reaction, the Y zeolite catalysts were completely black indicating the presence of highly aromatic coke. Analysis of the soluble coke revealed that this was indeed the case. The soluble coke molecules observed in the Y zeolite catalysts were polyaromatic compounds (Table 4). The same compounds were observed over all the Y zeolites studied. Coronene followed by benzoperylene were the major components; other molecules were present in small amounts. This clearly shows that the cages of zeolite Y have enough space to allow large molecules like coronene to form. The coke molecules were observed even after the catalyst was purged with an inert gas at 550°C, a temperature higher than their boiling points, which indicates that the coke is trapped inside the pores of the zeolite and is not present at the external surface. Analysis of soluble coke from a catalyst that was exposed to cyclopentane for a shorter time on stream (~6 h) showed much larger amounts of molecules, such as fluoranthene and benzofluorene than a catalyst that spent 100 h on stream. The number of aromatic rings in the coke molecules therefore gradually increased with time. Molecules with more aromatic rings than coronene were, however, not detected in the soluble coke.

Zeolite beta. The zeolite beta catalysts showed a very stable time-on-stream behavior (Fig. 5). The performance

of the beta-15 sample was remarkable, as the cyclopentane conversion remained close to 100% throughout the 100 h. The beta-8.5 sample showed a slow but continuous drop in activity throughout the time on stream, while in beta-30 the majority of the deactivation occurred during the

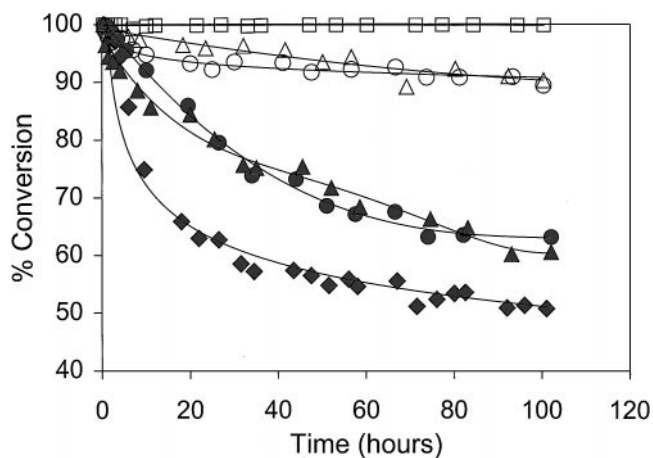


FIG. 5. Time-on-stream behavior of the zeolite beta and mordenite catalysts. □, beta-15; △, beta-8.5; ○, beta-30; ●, mor-35; ▲, mor-25; ◆, mor-10. WHSV = 3 h⁻¹, H₂/CP (molar) = 9, total pressure = 100 psig, T = 410°C, and 0.5% Pt loading.

TABLE 5
Product Selectivities (mol%) over the Pt/H-Beta and Pt/H-Mordenite Catalysts^a

	Initial (20 min)						Level-off stage					
	Beta-8.5	Beta-15	Beta-30	Mor-10	Mor-25	Mor-35	Beta-8.5	Beta-15	Beta-30	Mor-10	Mor-25	Mor-35
CP conversion	100.0	100.0	98.9	100.0	99.9	100.0	92.2	99.8	91.4	53.3	66.6	68.7
Methane	34.7	59.1	13.3	23.4	13.2	53.9	9.8	12.9	9.2	11.2	9.4	7.2
Ethane	18.1	27.9	10.1	22.4	12.9	22.2	6.7	11.9	6.2	11.3	7.9	5.0
Propane	31.1	11.9	29.8	38.5	33.7	17.9	23.5	32.6	17.4	28.8	16.9	14.4
2-Methylpropane	6.3	0.4	13.2	7.0	12.1	1.9	11.2	10.1	9.4	11.5	8.2	9.8
Butane	6.7	0.4	11.8	7.2	12.5	2.5	8.6	11.8	7.1	5.8	7.4	7.9
2,2-Dimethylpropane	0.1	0.0	0.3	0.0	0.0	0.0	0.1	0.5	0.3	0.0	0.0	0.0
2-Methylbutane	1.9	0.2	12.2	1.0	9.4	1.0	21.9	12.6	26.9	14.4	24.7	26.8
Pentane	1.1	0.1	8.2	0.4	6.1	0.4	15.1	7.7	20.0	8.4	19.1	21.4
2-Methylpentane	0.0	0.0	0.2	0.0	0.1	0.0	0.4	0.0	0.8	0.4	0.5	0.8
3-Methylpentane	0.0	0.0	0.1	0.0	0.0	0.0	0.3	0.0	0.4	0.2	0.3	0.4
Hexane	0.0	0.0	0.1	0.0	0.0	0.0	0.3	0.0	0.4	0.2	0.3	0.4
Methyl cyclopentane	0.0	0.0	0.1	0.0	0.0	0.0	0.3	0.0	0.3	1.6	1.3	1.4
Benzene	0.0	0.0	0.3	0.0	0.0	0.0	0.7	0.0	0.9	2.9	2.5	2.7
Toluene	0.0	0.0	0.2	0.0	0.0	0.0	0.9	0.0	0.6	2.4	1.2	1.5

^a WHSV = 3 h⁻¹, H₂/CP (molar) = 9, total pressure = 100 psig, T = 410°C, and 0.5% Pt loading.

initial few hours. Even though the beta-15 catalyst gave complete conversion of CP, a change in product selectivity with time was observed. At the initial stages, the product distribution showed a large fraction of cracked products; however, the cracking activity decreased with time, and a large amount of pentanes were observed at the level-off stage (Table 5). There was also a large drop in the amount of methane produced. These data indicate that metal and acid functions deactivated to a small extent but were not severe enough to cause a drop in cyclopentane conversion. Again, as in Y zeolites, the number of acid sites had a major effect on the catalyst performance rather than the nature of the acid sites (Table 3). The amount of coke deposited in the zeolite beta catalysts (Fig. 2) decreased with increase in the Si/Al ratio, but beta-8.5 showed a much larger amount of coke than the other beta zeolites. In addition to the high density of acid sites, the lower metal dispersion in beta-8.5 could have resulted in the deposition of a substantially higher amount of coke. In both of the used zeolite beta catalysts approximately 50% of the acid sites remained accessible to ammonia after 100 h on stream (Fig. 3). Even though a significant amount of coke was deposited in zeolite beta, the catalyst was able to maintain its activity. This shows that the three-dimensional structure of zeolite beta, which does not have any supercages or cavities, is highly resistant to deactivation.

Similar to the trend observed in Y zeolite, the metal dispersion in the low Si/Al beta (beta-8.5) sample was also relatively low. The metal function in the beta-15 catalyst was very active and showed a very high selectivity for methane during the initial period of the reaction, which resulted in high values for the C₁/C₃ ratio (Fig. 6). However, this ratio decreased rapidly indicating that the metal function was

deactivating faster than the acid function. Deactivation of metal during the initial period of the reaction could have occurred as a result of agglomeration of Pt upon contact with the hydrocarbon (18). In all the three beta catalysts the final value for the C₁/C₃ ratio was in the range of 0.4, which indicates that the activity of the acid function was being maintained and there was good balance between the two functions. From the product selectivity table for the beta zeolites (Table 5) it can be observed that no aromatics or compounds larger than C₅ were obtained with the beta-15 catalyst. As mentioned earlier, these molecules were formed by the cracking of small coke molecules. Therefore this suggests that formation of the coke precursor

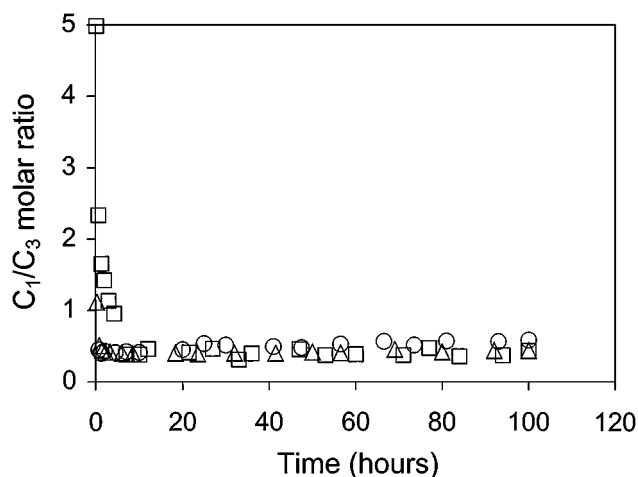


FIG. 6. Variation of C₁/C₃ molar ratio with time for beta zeolites. □, beta-15; ○, beta-8.5; △, beta-30. WHSV = 3 h⁻¹, H₂/CP (molar) = 9, total pressure = 100 psig, T = 410°C, and 0.5% Pt loading.

(cyclopentadiene) occurs to a very small extent. The metal is being maintained in a state that favors ring opening of cyclopentane rather than the dehydrogenation of cyclopentane to cyclopentadiene, thus limiting the coke formation reaction. This can happen due to differences in the electronic structure of the metal. The size of the metal cluster in the zeolite is known to greatly affect the type of reaction catalyzed by the metal function (19–21).

The soluble coke extracted from the zeolite beta catalysts was also analyzed by GC/MS. The coke mainly consisted of long-chain paraffinic or olefinic compounds and compounds with a long alkyl chain attached to a benzene ring. Polyaromatic coke molecules were surprisingly absent, even though the pores of zeolite beta were large enough to allow easy formation of these compounds. This observation again supports the earlier proposition that the state of the metal in zeolite beta decreased the formation of molecules with condensed aromatic rings to a great extent by minimizing the formation of cyclopentadiene. Only the coke molecules deposited in the beta-8.5 and beta-15 catalysts could be identified. The amount of soluble coke over beta-30 was too low to allow detection, even after concentration of the coke extract.

Mordenite. Acidic mordenite was reported to be highly susceptible to coking and deactivation in cracking reactions (5). This was attributed to its pore structure, since larger hydrocarbon molecules can diffuse in only one direction in its pore system. However, for this particular reaction the mordenite samples studied showed reasonably good stability (Fig. 5). This is mainly because in hydroconversion reactions the coking rates are slower, since coke can be hydrogenated and desorbed. Dealuminated mordenite samples performed better than the parent sample due to the lower acid site densities. As observed in zeolites Y and beta, the amount of hard coke deposited was lower in the catalysts with a lower acid site density (Fig. 2). Also, the fraction of acid sites remaining accessible to ammonia after reaction was higher in the catalysts with a lower acid site density (Fig. 3). There is again no correlation of the Brønsted/Lewis ratio with metal dispersion and catalyst performance (Table 2).

Mordenite is known to possess very strong acid sites, which we also observed in our STPD experiments. Consequently, all the mordenite samples studied showed a very high cracking activity during the initial stages (Table 5), which was maintained to a large extent even after 100 h on stream. The variation of C_1/C_3 ratios with time for the mordenite catalysts is very similar to that for the beta zeolites (Fig. 7), indicating that a good balance between the metal and acid functions can be achieved in catalysts having a Si/Al ratio in this range. In the initial stages, no aromatics or compounds larger than cyclopentane were observed in the product stream; however, a reasonably large amount of aromatics were observed in the later stages. This means that

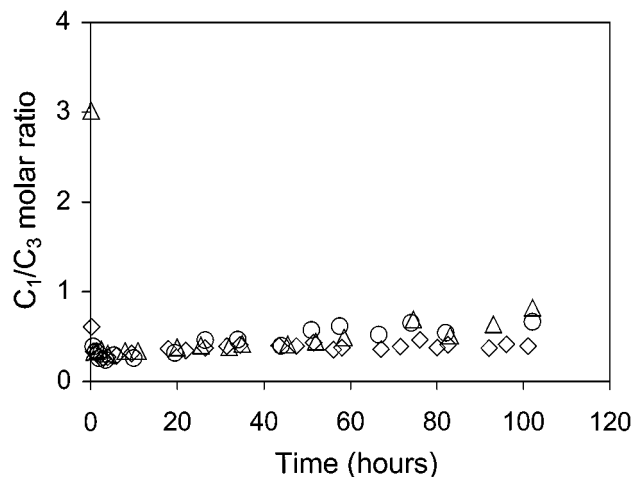


FIG. 7. Variation of C_1/C_3 molar ratio with time for the mordenite samples. Δ , mor-35; \circ , mor-25; \diamond , mor-10. WHSV = 3 h^{-1} , H_2/CP (molar) = 9, total pressure = 100 psig, $T = 410^\circ\text{C}$, and 0.5% Pt loading.

unlike the beta-15 sample, the metal function in the mordenites catalyzes dehydrogenation of CP to a significant extent, which eventually leads to polyaromatic coke. A large number and a wide variety of compounds were observed in the soluble coke extracted from the mor-10 sample as shown in Table 4. The coke consisted of polyaromatic compounds similar to those observed in zeolite Y. Long-chain paraffins, olefins, and long alkyl chains attached to one or two aromatic or cyclohexane rings, somewhat similar to the coke in zeolite beta, were also observed. The absence of aromatics in the product stream during the initial stages and the presence of both aliphatic and polyaromatic coke indicate that the state and therefore the selectivity of platinum in mordenite are changing with time. However, polyaromatic molecules with more than four aromatic rings were not observed in the soluble coke, which shows that there is no space in the pores of mordenite for molecules such as coronene to form.

L zeolite. The time-on-stream behavior of the L zeolite sample studied (LTL-3.5) was very similar to that of the Y-2.5 catalyst (Fig. 8). L zeolite is one dimensional but has expansions that are much larger than its pore opening, which makes its structure somewhat similar to that of zeolite Y. The combination of this pore structure and high density of acid sites severely affects the stability of L zeolite. The amount of coke deposited (Fig. 2), the variation of the C_1/C_3 ratio with time (Fig. 9), the product distributions (not shown), and the composition of soluble coke (Table 4) are similar to those observed with Y-2.5, indicating that L zeolite deactivates in the same manner as zeolite Y. The behavior of a dealuminated L zeolite sample (not shown, Si/Al = 6) was also similar to that of the parent sample and showed rapid and complete deactivation. As mentioned earlier, the dealumination was carried out

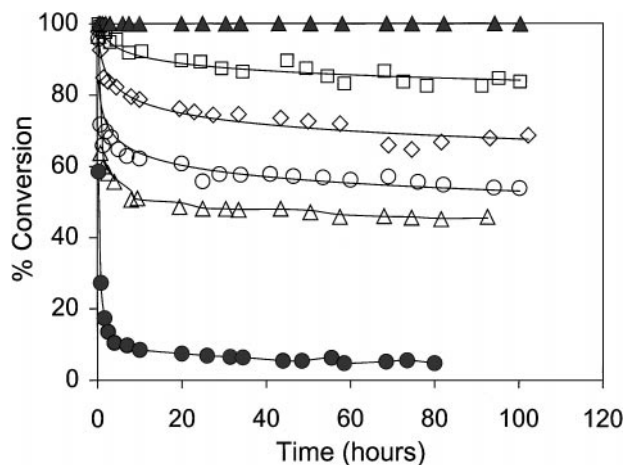


FIG. 8. Time-on-stream behavior of the ZSM-12, L zeolite, and ZSM-5 catalysts. ▲, ZSM-5-40; □, ZSM-12-38; ◇, ZSM-12-43; ○, ZSM-12-58; △, ZSM-12-80; ●, LTL-3.5. WHSV = 3 h⁻¹, H₂/CP (molar) = 9, total pressure = 100 psig, T = 410°C, and 0.5% Pt loading.

by steaming the zeolite followed by ammonium hexafluorosilicate (AHF) leaching. Steaming caused a partial loss of crystallinity, while AHF leaching is known to produce deposits of silica near the external surface of the zeolite crystal thereby decreasing the accessible pore volume (22). These factors are responsible for the very fast deactivation of the dealuminated L zeolite.

ZSM-12. The time stability of four different directly synthesized ZSM-12 samples with Si/Al ratios ranging from 38 to 80 was examined. The product selectivities obtained over these catalysts are given in Table 6. ZSM-12 also has a one-dimensional pore system but shows a better time stability than mordenite (Fig. 8). This remarkable stability of ZSM-12 despite its one-dimensional structure was first ob-

served in our group and it was shown that this is true for both naphtha-reforming and hydroisomerization reactions (14, 23, 24). Although ZSM-12 has a 12-member-ring pore, the size of the pore is intermediate to that of medium- and large-pore zeolites, which gives some shape-selective character to it. Also, ZSM-12 possesses a straight tube-like pore that does not have any cavities or channel intersections. The combination of these factors is responsible for the good time stability of ZSM-12.

The coking resistance of ZSM-5 due to its shape-selective behavior has been very well documented in the literature. Therefore, for comparison purposes a reaction was carried out using a ZSM-5 sample with a Si/Al ratio of 40, and it performed as expected. The ZSM-5-40 sample studied showed hardly any drop in conversion. This unique stability of ZSM-5 is well known, and the stability of the catalyst used in this experiment resulted from the combination of its pore structure and high Si/Al ratio. The product distributions (not shown) were quite similar to that obtained over beta-15; the selectivity for the 2-methylbutane was higher due to the higher Si/Al ratio.

There is a large variation in the time stabilities of the ZSM-12 catalysts with change in the Si/Al ratio, and the trend is completely different from that of the other zeolites (Fig. 8). The sample with the lowest Si/Al ratio (ZSM-12-38) gives the best time-on-stream behavior. It is very surprising to observe that ZSM-12 samples with different Si/Al ratios show markedly different stabilities. It should be noted that all the samples show a high activity initially, but the extent of deactivation is greater for higher Si/Al ratios. The four samples studied were directly synthesized and had very similar crystallinities, and therefore the samples were free from nonuniformities introduced by dealumination methods as in zeolite Y. The differences in acidity characteristics

TABLE 6

Product Selectivities (mol%) over the Pt/H-ZSM-12 Catalysts^a

	Initial (20 min)				Level-off stage			
	ZSM-12-38	ZSM-12-43	ZSM-12-58	ZSM-12-80	ZSM-12-38	ZSM-12-43	ZSM-12-58	ZSM-12-80
CP conversion	100.0	99.5	95.8	97.6	83.9	66.7	55.4	46.9
Methane	39.3	23.6	11.8	28.2	5.6	5.0	5.1	13.4
Ethane	24.3	11.8	2.6	7.4	2.3	1.6	0.8	1.4
Propane	22.0	18.3	4.0	9.0	8.1	4.4	1.9	4.1
2-Methylpropane	2.9	2.9	1.0	2.3	3.0	2.0	1.1	2.1
Butane	6.0	8.2	2.9	5.2	3.4	2.5	1.3	2.8
2-Methylbutane	3.7	20.5	43.9	27.5	43.1	46.4	47.7	39.3
Pentane	1.6	14.3	33.5	19.9	31.9	35.6	40.4	32.7
2-Methylbutane	0.0	0.0	0.1	0.1	0.0	0.0	0.2	0.4
3-Methylbutane	0.0	0.0	0.1	0.1	0.0	0.0	0.1	0.2
Hexane	0.0	0.0	0.0	0.0	0.0	0.0	0.1	0.3
Methyl cyclopentane	0.0	0.0	0.0	0.0	0.0	0.3	0.3	0.7
Benzene	0.0	0.0	0.0	0.0	0.9	1.2	0.7	1.4
Toluene	0.0	0.0	0.0	0.0	0.4	0.4	0.2	0.9

^a WHSV = 3 h⁻¹, H₂/CP (molar) = 9, total pressure = 100 psig, T = 410°C, and 0.5% Pt loading.

and platinum dispersion were examined to determine the reason for this behavior. However, there is no consistent variation in the Brønsted/Lewis ratio, and the metal dispersion is good in all the samples (Table 3). It is clear that the changes in acid site density affect the metal/acid balance, thus causing the ZSM-12 catalysts to deactivate to different extents.

The plot of C_1/C_3 ratios with time for the ZSM-12 catalysts shows this effect more clearly (Fig. 9). As the Si/Al ratio of the zeolite increases, the metal function starts dominating, and the C_1/C_3 ratios become larger. However in ZSM-12-38, the sample that shows the best stability, the C_1/C_3 ratio approaches that of zeolite beta and mordenite. This behavior suggests that as we go to higher Si/Al ratios the amount of acid sites is too low to maintain a good metal/acid balance. Even the loss of a small number of acid sites results in a deviation from good balance and causes the metal function to predominate. Another interesting observation in the case of ZSM-12 catalysts was that the amount of hard coke in all the samples studied was very low (Fig. 2). Also unlike other zeolites, all the ZSM-12 catalysts had about the same amount of coke, and there was no variation with the Si/Al ratio. The similarity in the amount of coke deposited on the ZSM-12 and ZSM-5 catalysts (Fig. 2) confirms that the pores of ZSM-12 exhibit a shape-selective effect, thus preventing the formation and deposition of compounds with polyaromatic rings. The soluble coke in the ZSM-12 catalysts was extremely difficult to identify, even after concentration of the extract, due the very small amount deposited. However, one of the major components appeared to be a compound with a long alkyl chain attached to a cyclohexane ring, indicating that the soluble coke might be similar to that observed in zeolite beta.

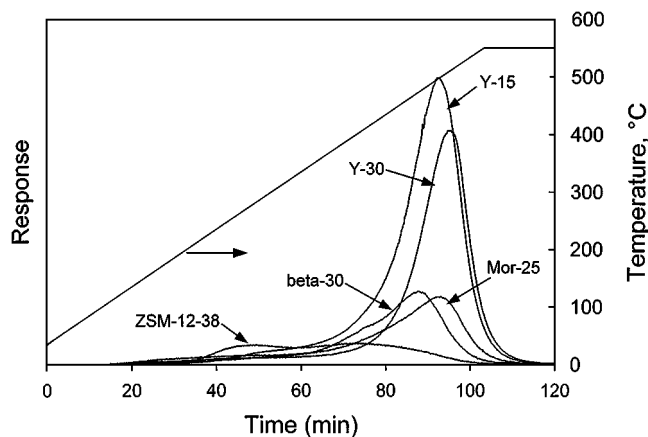


FIG. 10. Temperature-programmed oxidation of the coke deposited in selected catalysts after 100 h on stream.

TPO experiments were performed on selected deactivated catalysts to examine the combustion characteristics of the deposited coke and to obtain an idea about possible regeneration methods. The results are shown in Fig. 10. The peak maximum occurs at a temperature close to 500°C for all the catalysts except ZSM-12. It should be noted that all the catalysts shown in the figure were exposed to cyclopentane for 100 h on stream. In the case of ZSM-12, two peaks, one at a low temperature and one at a higher temperature, are obtained. However, the peak maxima occur at much lower temperatures compared to the other zeolites. A higher fraction of coke was burnt off at lower temperatures in beta zeolites also, indicating easier regeneration. With some of the catalysts, experiments were performed in which the cyclopentane flow was shut off but hydrogen was allowed to flow. The cyclopentane flow was started again after the hydrogen treatment. It was observed that in ZSM-12 and beta zeolites, this hydrogen treatment restored most of the activity, while it had little effect in the highly deactivated Y zeolite catalysts. These data show that in addition to showing good stability characteristics, ZSM-12 and zeolite beta are also easier to regenerate, the regeneration by hydrogen treatment being especially attractive.

Overall, considering all the zeolites it is observed that there is an optimum range of acidities for which a good balance between metal and acidic functions is obtained. In this study, this occurs over a fairly broad range of Si/Al ratios from 10 to 40 as indicated by the minimum in the C_1/C_3 ratios (Fig. 11). A minimum is observed for the Y zeolites also, although the C_1/C_3 ratios are higher than that of the other zeolites. The optimum range of Si/Al ratios roughly corresponds to number-of-platinum to number-of-acid sites ratio from 0.015 to 0.06. Alvarez *et al.* (25) observed a good stability for platinum sites/acid sites ratio >0.03 in the case of Y zeolites for hydrosiomerization and hydrocracking of alkanes; however, the ideal situation in their study occurred for much larger values of this ratio. For cyclopentane

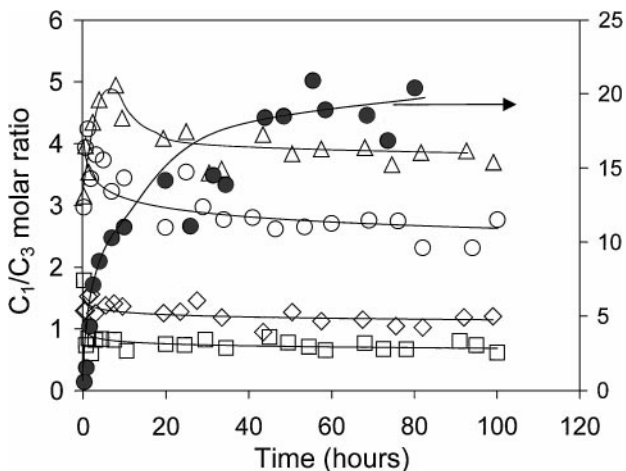


FIG. 9. Variation of C_1/C_3 molar ratio with time for ZSM-12 and LTL catalysts. \square , ZSM-12-38; \diamond , ZSM-12-43; \circ , ZSM-12-58; \triangle , ZSM-12-80; \bullet , LTL-3.5. WHSV = 3 h^{-1} , H_2/CP (molar) = 9, total pressure = 100 psig, $T = 410^\circ\text{C}$, and 0.5% Pt loading.

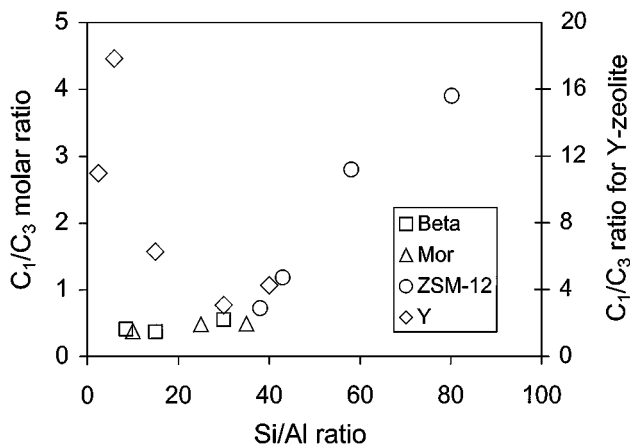


FIG. 11. C_1/C_3 molar ratio at the "level-off" stage for the various zeolites studied. A minimum in the C_1/C_3 ratio can be observed for zeolites with Si/Al roughly in the range from 10 to 40.

hydroconversion, in the zeolites with lower Si/Al ratios, the acidic function is very active initially and causes the formation of a large amount of coke. Figure 2 shows that low Si/Al zeolites have as much as three times the amount of coke compared to the high Si/Al samples. These coke molecules cover the acid sites and block access of the reactant to other acid sites resulting in deactivation. At Si/Al ratios higher than 40 the C_1/C_3 ratio again starts increasing, which suggests that the acid site density is not enough to maintain a good metal/acidity balance. The deactivation of acid sites in these catalysts allows the metal to dominate even further, and we observe a trend similar to that observed for the low Si/Al Y and L zeolites.

CONCLUSIONS

The various factors responsible for the deactivation of several Pt/H-zeolite catalysts have been thoroughly examined. Our results agree with literature reports that pore structure is the most important factor affecting coke formation and deactivation in zeolite catalysts. A three-dimensional pore structure without any cavities or cages (zeolite beta) was the best structure for resisting deactivation. However, in addition to the pore structure, the acid site density affects the amount of coke produced. Acid site density also affects the metal/acid balance of the catalyst and metal dispersion. Zeolites with Si/Al ratios between 15 and 40 had a good balance between the two functions and exhibited good stabilities. Polyaromatic coke was detected in zeolites Y, L, and mordenite, while the coke was mainly paraffinic in beta and ZSM-12. In ZSM-12 shape selectivity restricted the formation of polyaromatic coke. Even though

the pores of zeolite beta can accommodate polyaromatic compounds, the nature of coke was different, because the metal was being maintained in a state that favored opening of the CP ring rather than dehydrogenation, thereby limiting the reaction that produced polyaromatic coke.

ACKNOWLEDGMENTS

The authors acknowledge the support of the National Science Foundation through Award CTS-9702081. Acknowledgement is made to the donors of The Petroleum Research Fund, administered by the ACS, for support of this research through Grant ACS-PRF 31606-G5.

REFERENCES

1. Derouane, E. G., in "Catalysis by Acids and Bases" (B. Imelik, C. Naccache, G. Coudurier, Y. Ben Taarit, and J. C. Vedrine, Eds.), *Stud. Surf. Sci. Catal.* **20**, 221 (1985).
2. Rollmann, L. D., *J. Catal.* **47**, 113 (1977).
3. Rollmann, L. D., and Walsh, D. E., *J. Catal.* **56**, 139 (1979).
4. Walsh, D. E., and Rollmann, L. D., *J. Catal.* **49**, 369 (1977).
5. Guisnet, M., and Magnoux, P., *Appl. Catal.* **54**, 1 (1989).
6. Myers, C. G., Lang, W. H., and Weisz, P. B., *Ind. Eng. Chem.* **53**(4), 299 (1961).
7. Parera, J. M., Figoli, N. S., Beltramini, J. N., Churin, E. J., and Cabrol, R. A., in "Proceedings, 8th International Congress on Catalysis, Berlin, 1984," p. 593. Dechema, Frankfurt-am-Main, 1984.
8. Parera, J. M., Verderone, R. J., and Querini, C. A., in "Catalyst Deactivation 1987" (B. Delmon and G. F. Froment, Eds.), p. 135. Elsevier, Amsterdam, 1987.
9. Rosinski, E. J., and Rubin, M. K., U.S. Patent 3,832,449, 1974.
10. Ernst, S., Jacobs, P. A., Martens, J. A., and Weitkamp, J., *Zeolites* **7**, 458 (1987).
11. Mackey, J. R., and Murphy, W. J., *Zeolites* **5**, 233 (1985).
12. Zhang, W., Burckle, E. C., and Smirniotis, P. G., *Microporous Mesoporous Mater.* **33**, 173 (1999).
13. Beltramini, J. N., Martinelli, E. E., Churin, E. J., Figoli, N. S., and Parera, J. M., *Appl. Catal.* **7**, 43 (1983).
14. Zhang, W., and Smirniotis, P. G., *Appl. Catal. A* **168**, 113 (1998).
15. Guisnet, M., and Magnoux, P., *Catal Today* **36**, 477 (1997).
16. Remy, M. J., Stanica, D., Poncelet, G., Feijen, E. J. P., Grobet, P. J., Martens, J. A., and Jacobs, P. A., *J. Phys. Chem.* **100**, 12,440 (1996).
17. Parera, J. M., Figoli, N. S., Traffano, E. M., Beltramini, J. N., and Martinelli, E. E., *Appl. Catal.* **5**, 33 (1983).
18. Zhang, Z., Lerner, B., Lei, G.-D., and Sachtler, W. M. H., *J. Catal.* **140**, 481 (1993).
19. Gault, F. G., *Adv. Catal.* **30**, 1 (1981).
20. Sachtler, W. M. H., and Zhang, Z., *Adv. Catal.* **39**, 129 (1993).
21. Gates, B. C., in "Catalysis in Petroleum Refining and Petrochemical Industries 1995" (M. Absi-Halabi, Ed.), p. 49. Elsevier, Amsterdam, 1996.
22. Chauvin, B., Boulet, M., Massiani, P., Fajula, F., Figueras, F., and Courieres, T. D., *J. Catal.* **126**, 532 (1990).
23. Zhang, W., and Smirniotis, P. G., *J. Catal.* **182**, 400 (1999).
24. Zhang, W., and Smirniotis, P. G., *Catal. Lett.* **60**, 223 (1999).
25. Alvarez, F., Ribeiro, F. R., Perot, G., Thomazeau, C., and Guisnet, M., *J. Catal.* **162**, 179 (1996).